ORIGINAL PAPER

Ethiopian decadal climate variability

Mark R. Jury

Abstract Ethiopian decadal climate variability is characterized by application of singular value decomposition to gridded rainfall data over the period 1901–2007. Two distinct modes are revealed with different annual cycles and opposing responses to regional and global forcing. The northern zone that impacts the Nile River and underlies the tropical easterly jet has a unimodal rainy season that is enhanced by Atlantic Multidecadal Oscillation warm phase. This rainfall mode is linked with the Atlantic zonal overturning circulation and exhibits 10–12-year cycles through much of the twentieth century. The southern zone has a bimodal rainy season that is enhanced by Pacific Decadal Oscillation cool phase and the southern meridional overturning circulation. Multiyear wet and dry spells are characterized by sympathetic responses in the near-equatorial trough extending from Central America across the African Sahel to Southeast Asia. The interaction of Walker and Hadley cells over Africa appears to be a key feature that modulates Ethiopian climate at decadal frequency through anomalous north–south displacement of the near-equatorial trough.

M. R. Jury
University of Zululand,
KwaDlangezwa 3886, South Africa

M. R. Jury (✉)
Physics Department, University of Puerto Rico,
Mayagüez, PR 00681, USA
e-mail: jury@uprm.edu

1 Introduction

Climate variability influences all facets of human activity, particularly in agrarian economies. To ensure the sustainable use of resources, it is appropriate to develop climate predictions based on scientific understanding that is tailored to specific areas and impacts (Glantz et al. 1991; Glantz 1996; Moura and Sarachik 1997; WCRP 1999; Hammer et al. 2000; Jury 2002). The predictability of climate derives primarily from slowly evolving ocean conditions. Using sea surface temperature (SST) forecasts in coupled general circulation models, a measure of success has been achieved in forecasting African rainfall at one season lead time (Lyon and Mason 2009). Atmospheric variables may be skilful in climate prediction in the context of wind forced ocean Rossby waves and equatorial upwelling dynamics (Jury et al. 1997; Xie et al. 2002; Jury and Huang 2004).

The interaction of SST and atmospheric convection associated with the near-equatorial trough is an important driver of tropical climate variability. As the surface layer of the equatorial ocean cools under the influence of wind-driven upwelling and surface heat loss, atmospheric convection shifts. This alters the global circulation and hydrological budget over Africa (Lamb 1978, 1982; Nicholson 1981, 1998; Nicholson and Palao 1993; Nicholson and Grist 2001). Past studies have attributed African climate variability to meridional gradients of Atlantic SST (Folland et al. 1986; Lough 1986; Palmer 1986; Semazzi et al. 1996) and to the Pacific El Niño-Southern Oscillation (ENSO; Fontaine et al. 1995; 1998). During ENSO warm phase upper westerly winds prevail over the Central Atlantic. Downstream over Africa, these winds

descend, weakening the Hadley circulation (Hastenrath 2000; Camberlin et al. 2001). In addition to ocean-atmosphere coupling, land-atmosphere feedback on the boundary layer climate provides a forcing that has received attention (Charney 1975; Xue et al. 1990; Zeng and Eltahir 1998; Zeng et al. 1999).

While a majority of studies have concentrated on Africa's Sahel climate west of 20ºE, here, the focus is directed toward understanding decadal climate variability of the Ethiopian highlands, which impacts on the flow of the Nile River (Quinn 1992; Eltahir and Wang 1999; Wang and Eltahir 1999). Ethiopian climate variability has been related to ENSO and the Southwest monsoon over the Arabian Sea (Camberlin 1995, 1997; Camberlin et al. 2001). Deep convection over India establishes a temperature gradient that drives a tropical upper level easterly jet over the Arabian Sea (Segele et al. 2009). When the jet surges, boreal summer rainfall over Ethiopia tends to increase. Ethiopian rainfall is suppressed following an active tropical cyclone season in the Southwest Indian Ocean (Shanko and Camberlin 1998).

Fig. 1 1950–2000 data density for **a** SST measurements per month per 2º box and **b** GPCC rain gauges per 2º box. **c** Time series of GPCC rain-gauge density in Ethiopian highlands area (*box* in **b**)
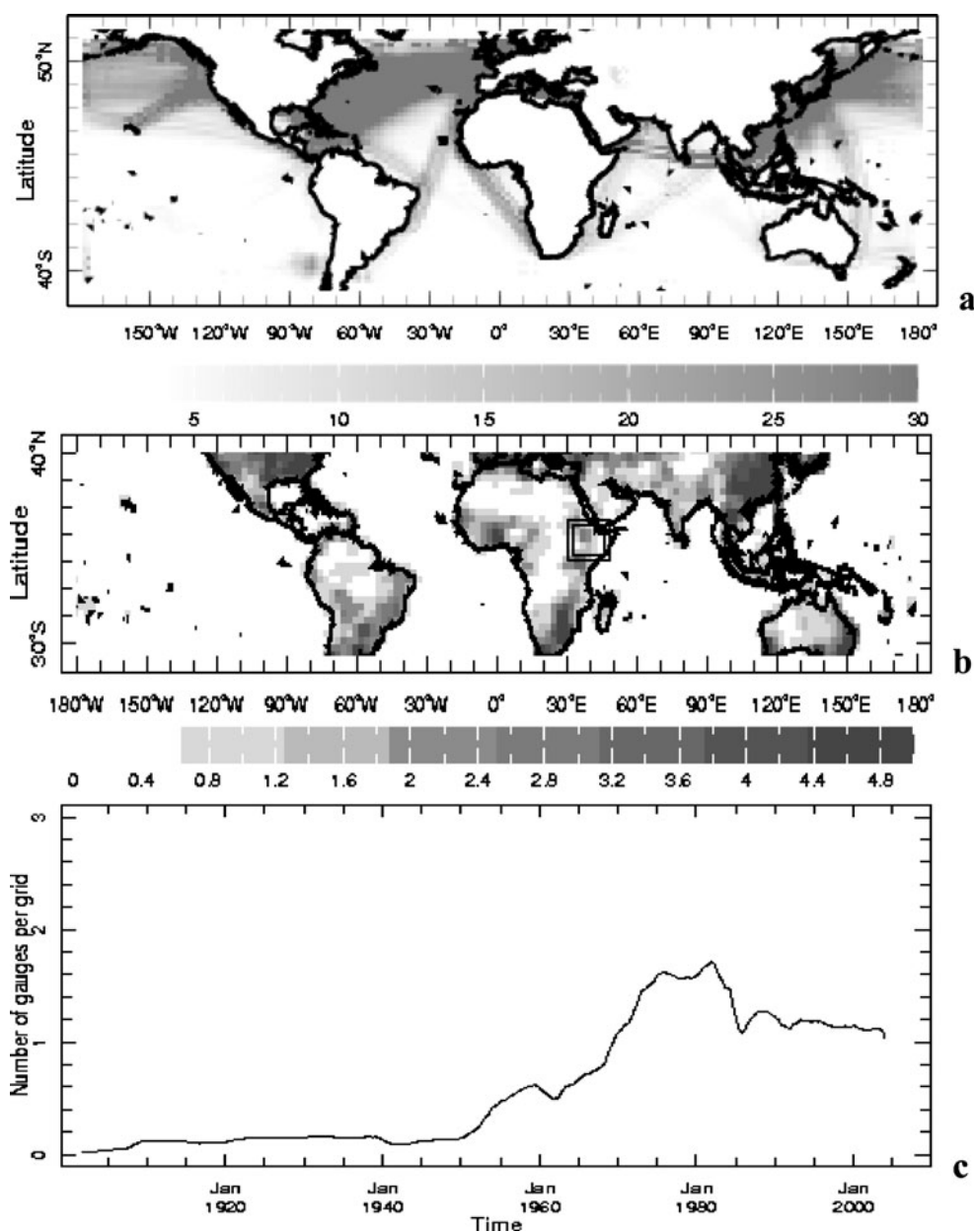
Fig. 2 a Topographic map of Africa with Ethiopia outlined, **b** mean 850 hPa winds in July and country names, **c** mean GPCC July rainfall in millimeter per month, **d** mean July vegetation fraction from satellite NDVI with *dashed line* for Rift Valley, **e** mean NCEP 500 hPa vertical motion (Pa/s) and winds in July, **f** Hovmoller time-longitude plot of mean NCEP 700 hPa relative humidity on 9° N, describing seasonal cycle
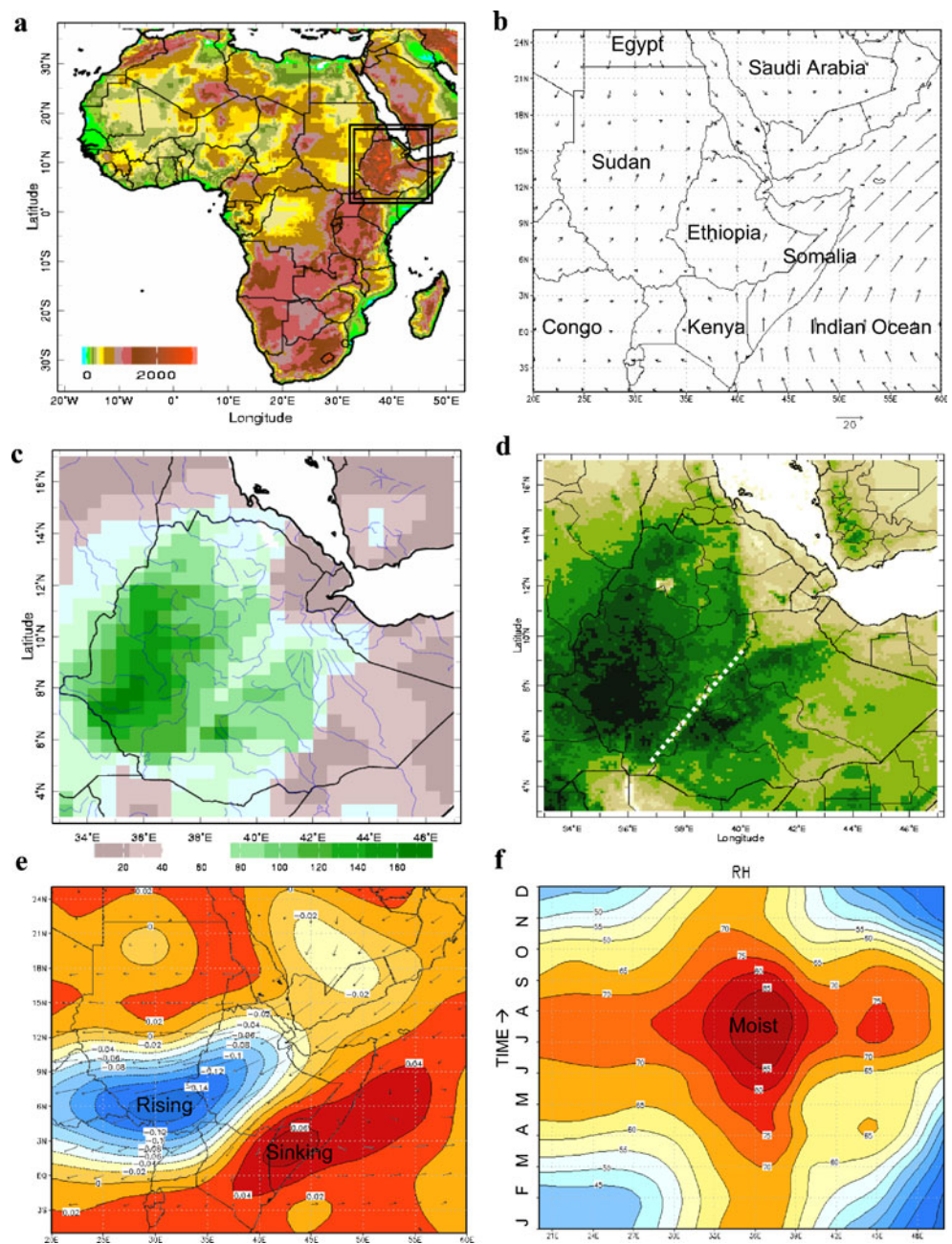
The objective of this paper is to understand the large-scale atmospheric circulations that modulate Ethiopian climate at decadal time scales during the twentieth century. The forcing mechanisms are studied through analysis of historical datasets and statistical analyses. Another goal of this study is to understand how the Walker and Hadley circulations interact over Africa, extending the earlier work of Yeshanew and Jury (2007). A number of scientific questions are addressed: (1) What are the characteristics of Ethiopia's decadal climate variability? (2) Which environmental fields are most important and how do they evolve? And (3) What role does the ocean play in the Walker–Hadley interaction? In Section 2, the data and methods are outlined. Section 3 provides results by analysis of mean climate, rainfall and vegetation modes, large-scale environmental factors, and composites for wet and dry summers. The conclusions are given in Section 4 within a conceptual framework.
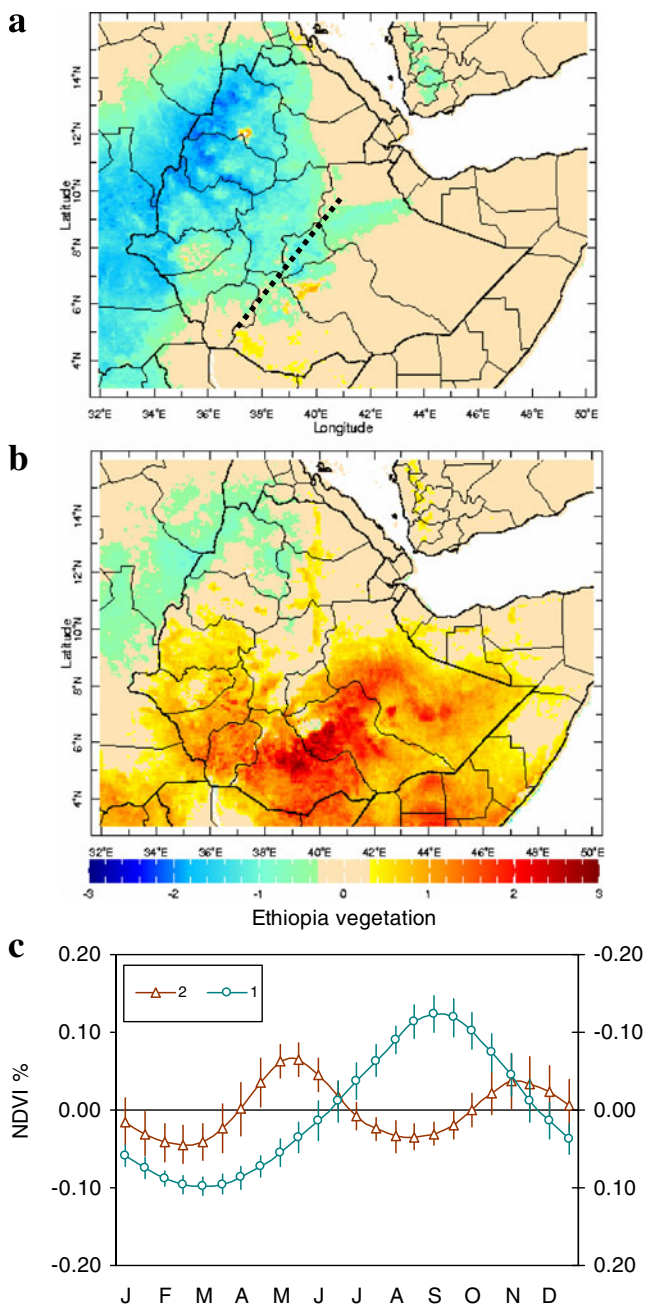
Fig. 3 **a** SVD loading pattern for mode-1 satellite vegetation, **b** SVD loading pattern for mode-2 satellite vegetation, and **c** mean mode-1 (*inverted*) and mode-2 time scores and standard deviations (*error bars*) contrasting the annual cycle. *Dashed line* in (**a**) is Rift Valley. Loading pattern *color bar* has units of normalized anomalies from −3 to +3

2 Data and methods

To study the climate of Ethiopia (3–17° N, 33–47° E, Fig. 1a) monthly gauge rainfall from the World Climate Research

Program Global Precipitation Climatology Center (GPCC), dataset is extracted from the International Research Institute's Climate Library over the period 1901–2007. Although GPCC rainfall records are quite complete and quality checked, data density in the period prior to 1950 is somewhat limited across Ethiopia (Conway et al. 2004, Fig. 1c). The GPCC monthly rainfall data are optimally interpolated to a 0.5° grid as described in Rudolf and Schneider (2005) to account for orographic effects. Here, the seasonal cycle is filtered out, and normalized rainfall anomalies are linearly detrended and smoothed with a centered 60-month running mean to eliminate high-frequency fluctuations and drift. The filter suppresses 3- and 6-year cycles which have been previously studied (Yeshanew and Jury 2007). To investigate the nature of climatic oscillations, the filtered rainfall time series are subjected to wavelet spectral analysis. The continuous 5-year filtered rainfall fields are objectively clustered using singular value decomposition (SVD) as described by Bretherton et al. (1992); von Storch and Navarra (1995); and Venegas (2001). SVD analysis involves an eigenvector decomposition of the covariance matrix within a single input field, such that the variability is reduced to modes of decreasing normalized variance. For each mode, there is a spatial pattern of loadings that describe its area of influence and time scores that reveal the amplitude and wavelength of oscillation. Varimax rotation is imposed to limit the effects of domain size.

In a similar manner, SVD is applied to monthly reanalyzed atmospheric fields (Kalnay et al. 1996) of National Center for Environmental Prediction (NCEP) zonal and meridional winds, and stream function in vertical sections averaged over the African hemisphere, and to NOAA-extended SST (Smith et al. 2008) with the same filtering, over the 1949–2007 time period. SVD is also applied to bimonthly satellite vegetation (NDVI) data in the period 1981–2004 to explore how the annual cycle affects the interaction between Ethiopian climate and surface vegetation, with filtering limited to a 3-month running mean (seasonal cycle is retained). To quantify the influence of (mainly NCEP) environmental variables on filtered Ethiopian rainfall, SVD time scores are used in lag cross-correlation. Correlation values >0.40 are considered significant at the 95% confidence limit for a degrees of freedom of ~22 (in the period 1949–2007) that takes into account the reduction of sample size by the 5-year filter.

Composite environmental conditions are evaluated on a seasonal basis, by ranking the top 10 wet and dry summers (May–October) based on GPCC data averaged over the Ethiopian highlands (4–14° N, 34–42° E). Wet summers

Fig. 4 **a** SVD loading pattern for mode-1 North Ethiopia 5-year filtered rainfall anomalies, **b** 5-year filtered temporal variability, and **c** wavelet spectra with cone of validity; **d** loading pattern for mode-2 South Ethiopia rainfall, **e** 5-year filtered temporal variability, and **f** wavelet spectra with cone of validity. *Color bar* for loading patterns as in Fig. 3. Units of **b**, **e** are converted to millimeters per month
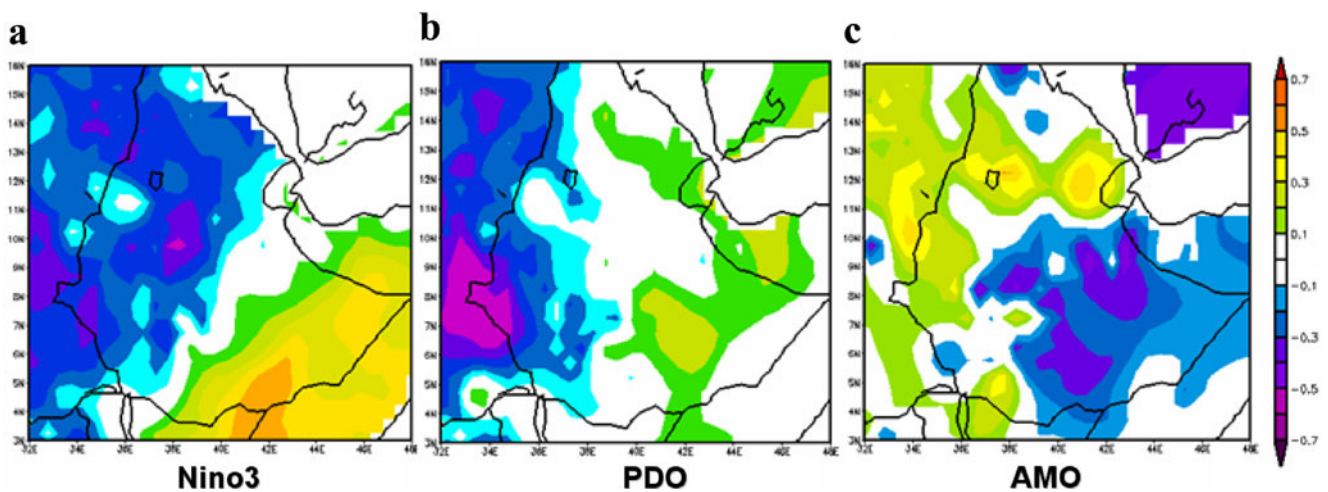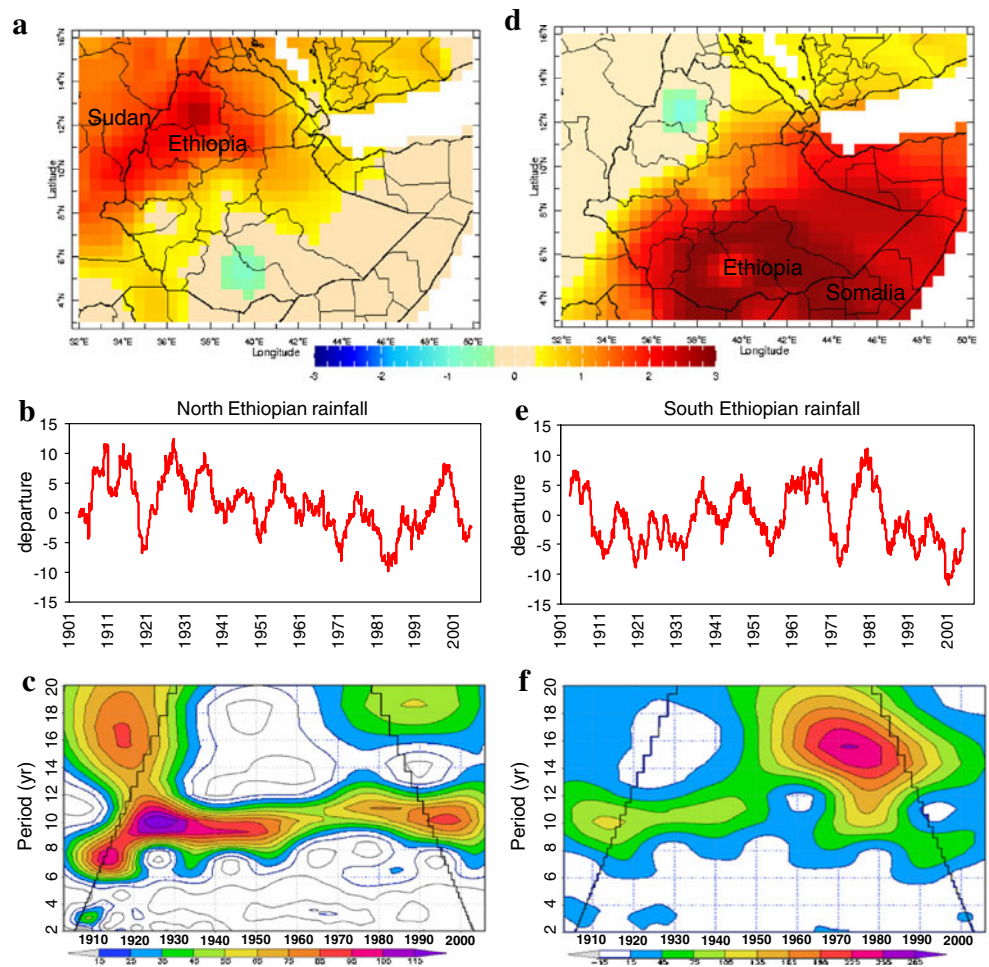
Fig. 5 Zero-lag correlation of unfiltered summer GPCC gauge rainfall 1949–2007 with various climatic indices: **a** Nino3, **b** Pacific decadal oscillation, and **c** Atlantic multi-decadal oscillation

Table 1 Cross-correlation of continuous 5-year filtered Ethiopian rainfall with filtered environmental SVD time scores in the period 1949–2007

	N.Eth-R	S.Eth-R
N.Eth-R		
S.Eth-R	−0.10	
psi1w	**−0.44**	0.07
psi2w	0.09	−0.32
psi3w	−0.29	**0.58**
U1w	**−0.52**	0.11
U2w	0.03	0.16
U3w	**0.43**	**−0.44**
psi1h	**−0.57**	0.20
psi2h	−0.09	**0.49**
psi3h	−0.11	0.13
V1h	**0.43**	−0.06
V2h	0.36	−0.24
V3h	0.18	**−0.70**
SST1	**0.53**	**−0.40**
SST2	0.05	0.30
SST3	-0.20	0.26
SST4	0.33	**−0.51**

Bold values are significant at 95% confidence limit with ~22 *df*, numbers refer to modes

R rainfall, *psi* stream function, *U* zonal wind, *V* meridional wind, *w* east–west section, *h* north–south section

include: 1959, 1962, 1963, 1965, 1966, 1979, 1998, 1999, 2006, and 2007. Dry summers are 1971, 1972, 1973, 1984, 1985, 1986, 1992, 2002, 2003, and 2004. The global structure of GPCC rainfall, NOAA-SST, and NCEP upper winds are analyzed by subtracting dry seasons from wet. This helps place Ethiopian decadal climate variability in a wider context. The composite structure of humidity, vertical motion, and zonal and meridional overturning circulations is studied as vertical sections over Africa.

Figure 1a–c addresses the issue of data density. The map of ship-based SST measurements in the period since 1950 indicates that the North Atlantic and main shipping lanes are well covered. Elsewhere, less data are available. The rain gauge network (Fig. 2b) is adequate for the study of decadal climate variability across most land areas, and Ethiopia appears to be no worse than more developed regions. Yet, coverage is limited prior to 1950 (Fig. 1c). To overcome this problem, modern satellite patterns are projected onto historical data to create realistic patterns, using optimal interpolation methods similar to SVD. In this way, the Ethiopian climate can be linked in time and space with surrounding information to create a more complete coverage that can be analyzed as described here. SVD has the value of picking up more recent patterns when the data density is high and projecting them back in time over the period of lower data density. The 5-year filter also helps close data gaps without the need to artificially supplement the record.

3 Results

3.1 Modes of Ethiopian climate

Ethiopia is elevated ~2,000 m above the surrounding areas (Fig. 2a), and orographic forcing of convection is common (Fig. 2c). During summer, the southwest monsoon blows along the coast of Somalia (Fig. 2b). It instills cyclonic vorticity and helps draw tropical air from the Congo Basin to the Ethiopian highlands, where vegetation cover is dense (Fig. 2d). Over Southern Sudan, there is a region of rising motion at 500 hPa that extends into western Ethiopia (Fig. 2e) along the axis of easterly flow. Although moisture is present over Ethiopia through most of the year (Fig. 2f), it is most zonally extensive in midsummer (July) when a zonal trough lies across the region. During this season, the Indian Monsoon generates an upper easterly jet that triggers pulses of rainfall. Easterly waves are initiated over the Ethiopian highlands from May to October (Lin et al. 2005) and propagate across the African Sahel into the tropical Atlantic.

The leading SVD modes for vegetation in the period 1981–2004 are illustrated in Fig. 3a–c, with seasonal cycle and high-frequency variability retained. Mode 1 is represented as a cluster over Northwestern Ethiopia that extends into Sudan. Its time score has a 12-month cycle, indicating that rainfall from vortices in the near-equatorial trough reach this latitude by midsummer and retreat thereafter. Vegetation in Northwestern Ethiopia is least productive in February–March and gradually rises to a peak in August–September. Mode 2 clusters over the southern half of Ethiopia and extends into Northern Kenya. It exhibits a 6-month cycle related to early and late summer rainfall maxima inducing two distinct seasons of vegetation growth, typical for near-equatorial zones. Inspection of the mean time score error bars representing the standard deviation (Fig. 3c) reveals that the early summer vegetation peak (April–May) is less variable than late summer (October–November). The vegetation SVD analysis divides Ethiopia into two climatic regimes: northwestern unimodal and southern bimodal. The question is whether climate variability should also separate along these lines.

GPCC rainfall modes in the period 1901–2007 (Fig. 4a, d) feature a cluster in the north as mode 1 and a cluster in the south as mode 2, representing 19% and 13% of total variance, respectively. Hence, the vegetation modes correspond with rainfall despite differences in filtering and time period. The northern mode-1 cluster extends westward into Sudan. The southern mode-2 cluster reaches eastward into Somalia. Time scores for

the filtered rainfall SVD modes are given in Fig. 4b, e and wavelet spectral analysis highlights the amplitude and wavelength in Fig. 4c, f. Northern Ethiopian rainfall displays a persistent decadal cycle throughout the twentieth century, as found earlier (Wood and Lovett 1984; Seleshi et al. 1994). Southern Ethiopian rainfall, on the other hand, has a weak 10–12-year cycle early in the record, and a 14–18-year cycle in the period 1950–1990. Inspection of spectral energy in unfiltered rainfall records suggests that the decadal oscillations are a real feature and not a statistical artifact. When area averages of 5-year smoothed rainfall in the two regions are analyzed, their time series are uncorrelated ($r=-0.10$). This is seen as a

strategic advantage for Ethiopia: different parts of the same country have independent climatic regimes.

3.2 Environmental links

Mapping the correlation of global climate indices onto gridded GPCC summer (May to October) rainfall time series, the opposing character of rainfall regimes in northern and southern Ethiopia emerges. Of a possible 30 indices available from the NOAA Climate Diagnostics Center, three achieve robust associations in the period 1949–2007 (Fig. 5a–c). Pacific SST Nino3 correlations are significantly negative northwest of the

Fig. 6 SVD loading patterns for **a** vertical N–S section mode-1 stream function (PSI-1) and **b** mode-3 meridional wind (V-3); SVD loading maps for **c** mode-1 SST and **d** mode-2 SST; 5-year filtered time score comparison between **e** Northern and **f** Southern Ethiopia rainfall and leading environmental modes; lag-correlation plot between **g** PSI-1 and Northern Ethiopia rainfall and **h** V-3 and Southern Ethiopia rainfall. Positive values on X-axis (**g**, **h**) refer to variable leading rainfall. Environmental variable refers to left-hand inverted Y-axis in (**e**, **f**)
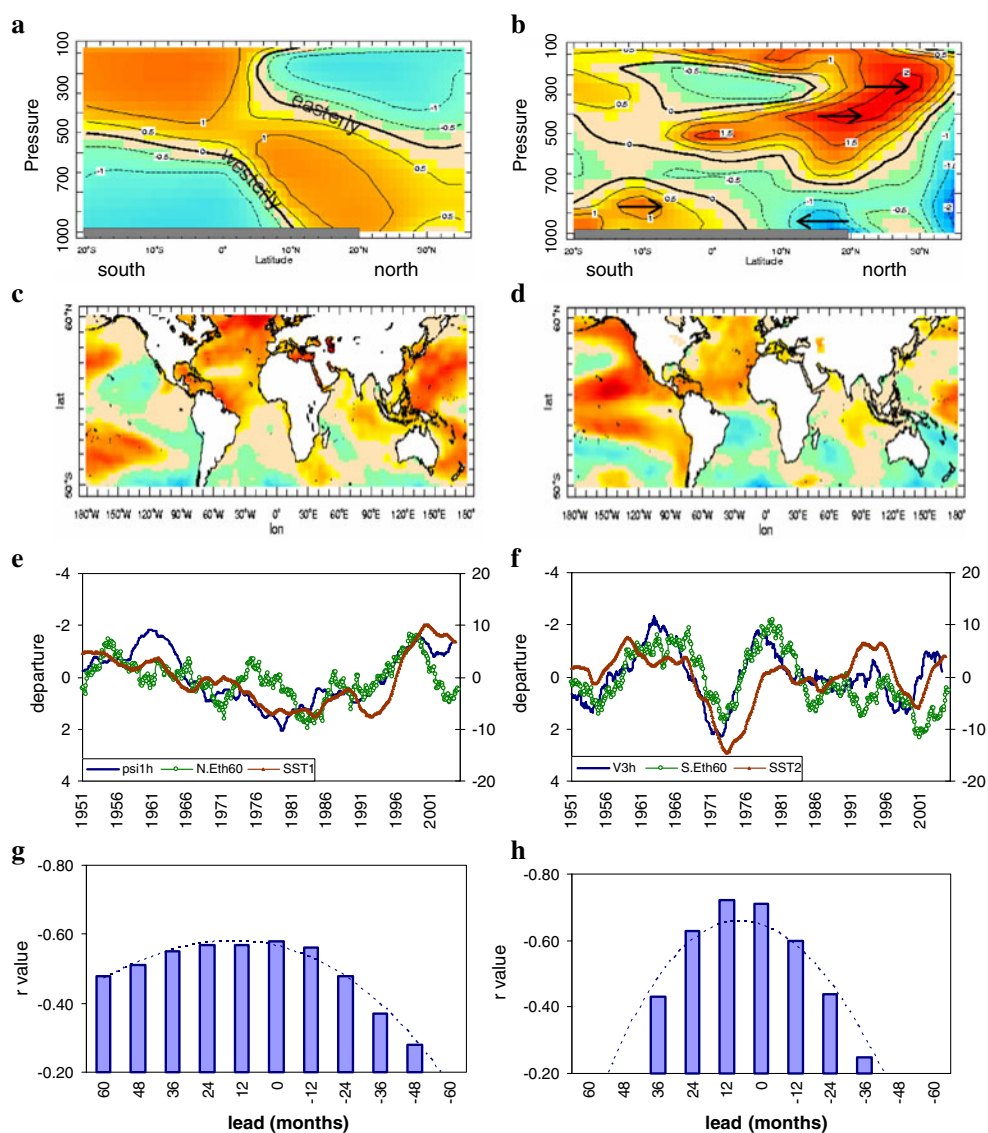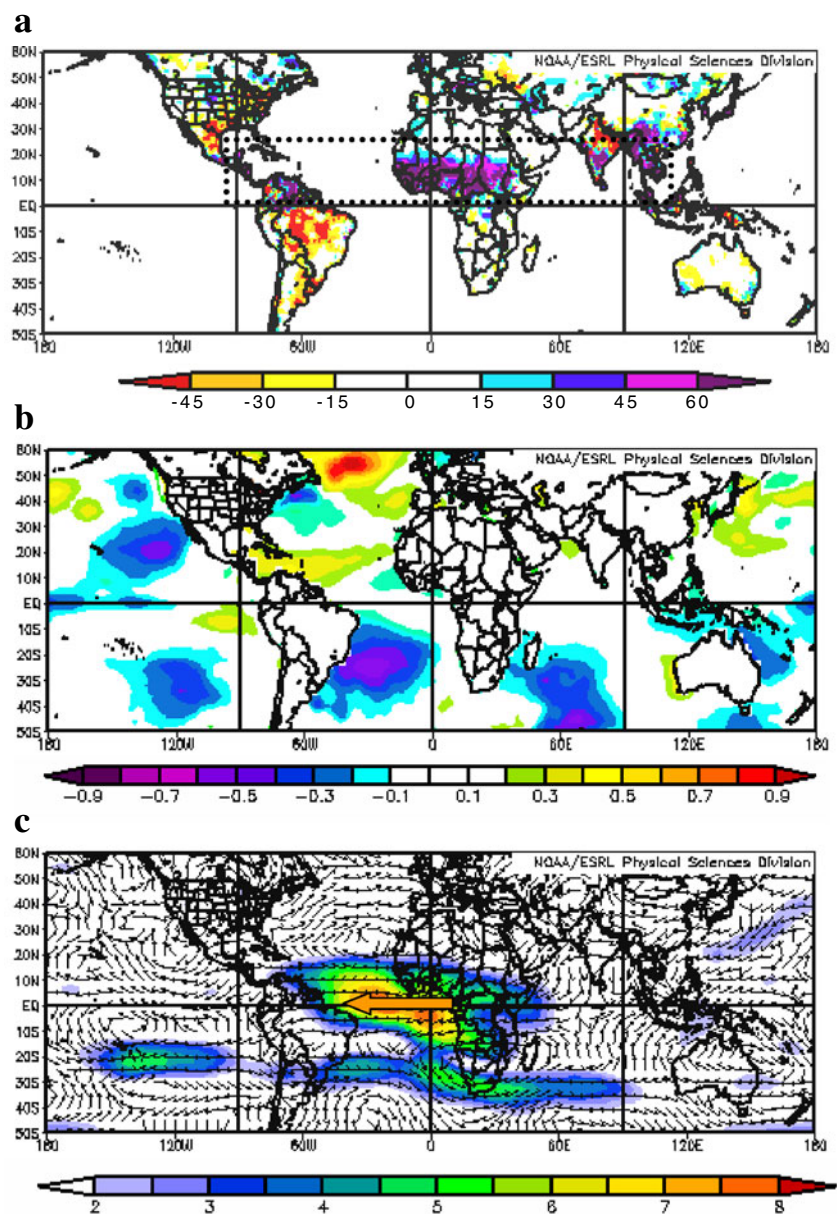
Rift Valley and positive to the southeast. Hence, ENSO warm phase may be associated with a reduced northward migration of the ITCZ, such that rainfall is confined near the equator. Pacific SSTs are also known to modulate the zonal Walker Circulation over the Indian Ocean, which in turn affects the end of the rainy season in southern Ethiopia. The Pacific Decadal Oscillation (PDO, Tourre et al. 1999; Barlow et al. 2001) also exhibits a strong negative correlation northwest of the Rift Valley and weak positive association to the southeast. The Atlantic Multidecadal Oscillation (AMO, Enfield et al. 2001) correlation pattern is reversed: warm phase enhances rainfall in northwest districts and suppresses to the southeast.

The zonal and meridional overturning atmospheric circulations are characterized over the African hemisphere by application of SVD to NCEP U and V wind components and stream function in vertical sections from 1,000–100 hPa averaged over the latitudes 10° N–5° S for east–west sections and longitudes 60° W to 90° E for north–south sections. In addition, SVD is applied to NOAA SST fields, with consistent filtering (e.g., detrended anomalies with 5-year running mean). Patterns that correspond with Ethiopian rainfall variability are shown in Fig. 5a–h, while cross-correlations are listed in Table 1.

Ethiopian rainfall modes 1 and 2 relate to north–south sections of stream function and meridional wind, respectively. The stream function (psi) SVD loading

Fig. 7 Composite wet minus dry differences in respect of Ethiopian rainfall for **a** gauge rainfall (mm/month), **b** SST (°C), and **c** 150 hPa wind (m/s). *Dashed box* in (**a**) highlights zone of anomalous rainfall and near-equatorial trough

pattern is tilted such that the low level cyclonic maximum underlies the upper level anticyclonic maximum, reflecting a Walker Circulation across the African hemisphere (Fig. 6a). The time scores correspond ($r = -0.57$, Fig. 6e) and lag-correlations remain significant to 36-month lead time (Fig. 6g). This linkage is consistent with SST mode 1 (Fig. 6c) that reflects the AMO ($r = -0.83$). Southern Ethiopian rainfall mode 2 is well correlated with meridional wind mode 3 (Fig. 6b, Table 1). The filtered SVD time scores correspond ($r = -0.70$) with lag-correlations significant to 24-month lead time (Fig. 6h). The association is modulated by SST mode 2 (Fig. 6d) that reflects the PDO ($r = -0.60$). The SVD time score correlations (Table 1) suggest that the Hadley circulation helps activate rainfall over southern Ethiopia. Although correlation values are inflated by the 5-year filter, the structure of the lag-correlation function is informative. It suggests multiyear predictive potential from atmospheric derivatives that characterize the global overturning circulations. SST modes and indices, on the other hand, seem to lag the overturning atmospheric circulations in the decadal band.

3.3 Composite differences

While the continuous 5-year filtered SVD rainfall analysis has revealed certain aspects of Ethiopia's decadal climate variability, it is useful to place the work into a wider context using seasonal data. In this regard, composites were constructed by averaging fields for the top 10 dry and wet summers (May–October) since 1949 and subtracting to obtain the difference. Results are given in Fig. 7a–c for rainfall, SST, and upper winds. Rainfall is found to increase >30 mm/month across the 0–20º N zone influenced by the near-equatorial trough, from Central America eastward across the African Sahel and Southern India to Southeast Asia. SST differences are below normal across the southern subtropics in the vicinity of the semi-permanent anticyclones. The extra-tropical Pacific exhibits negative SST differences in a PDO pattern, while the North Atlantic has positive differences consistent with AMO warm phase. The upper wind field in respect of Ethiopian wet minus dry conditions is strongly easterly (10 ms^{-1}) over the Central Atlantic and consistent with Walker circulation adjustment to ENSO/PDO cool phase (Yeshanew and Jury 2007).
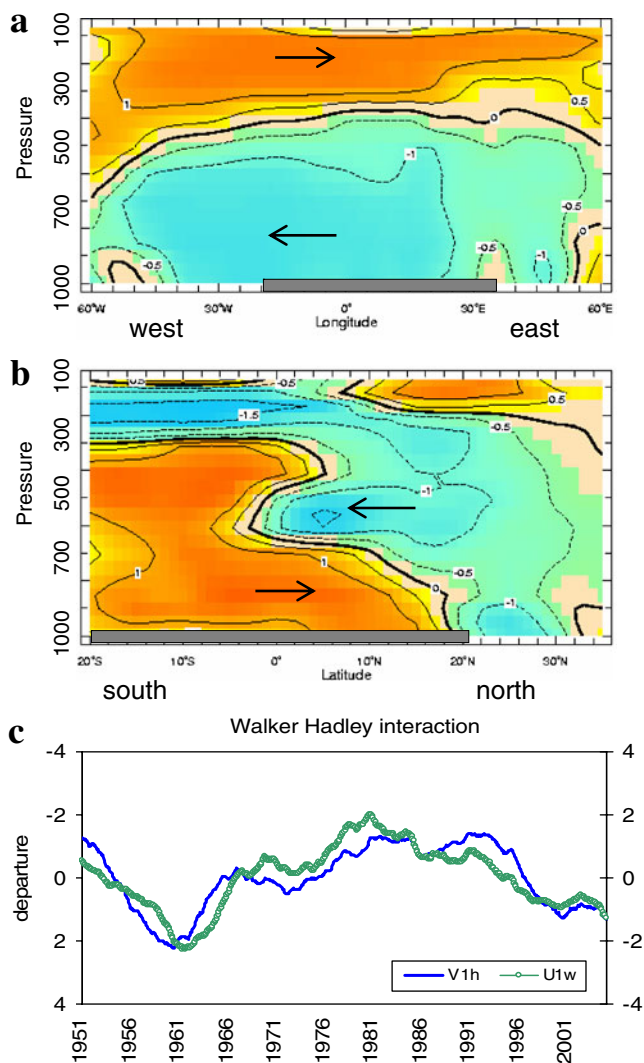

Fig. 8 Vertical north–south section composite wet minus dry differences in respect of Ethiopian rainfall for: **a** specific humidity (g/kg), **b** omega (Pa/s), **c** meridional wind (m/s) representing southern Hadley cell, **d** zonal wind (m/s) representing Atlantic Walker cell, **e** meridional wind 2 years prior, **f** zonal wind 2 years prior, all averaged over African longitudes 20° W to 50° E
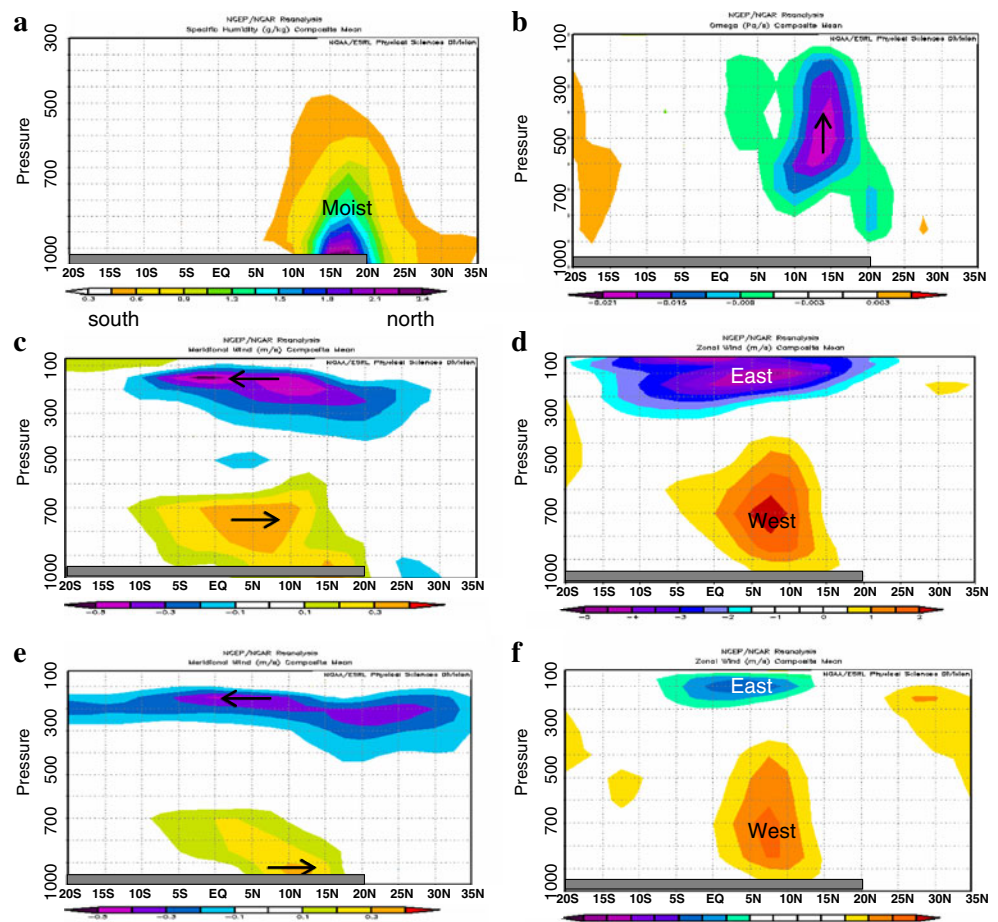
Vertical north–south sections are constructed over African longitudes for the wet minus dry summer (May–October) composite and illustrated in Fig. 8. Moisture is enhanced in the 1,000–500 hPa layer from 15–20° N (Fig. 8a) and suggests a northward displacement of the near-equatorial trough in conjunction with rising motion over the northern Sahel (Fig. 8b). Spin-up of the southern Hadley cell is evident in meridional wind differences over the equator (Fig. 8c): southerly in the low levels (+V, 800–600 hPa) and northerly in the upper levels (−V, 200–150 hPa). The anomalous southern Hadley circulation coincides with upper easterly (–U)/lower westerly (+U) wind differences associated with the Atlantic Walker cell (Fig. 8d). Analyzing differences in the zonal and meridional overturning circulations, it is found that they are well

established 2 years before anomalous summer rains are observed over the Ethiopian highlands (Fig. 8e, f). This is not an artifact of filtering but a reflection of the slow rhythm in overturning circulations that modulate decadal climate variability.

While the composites have indicated how the atmospheric circulations relate to tropical rainfall, an objective SVD analysis of zonal and meridional wind sections reveals how the low frequency component of the Walker and Hadley cells interact over Africa (Fig. 9). The mode-1 Walker circulation across the Atlantic corresponds closely with the mode-1 Hadley circulation over Africa ($r=-0.85$). When upper westerlies/lower easterlies are established, meridional convergence in the lower branch of the Hadley cell is suppressed. The time scores (Fig. 9c) indicate the Hadley cell leads by about 1 year in the 1950–1980 period and lags by a few months thereafter. Although Walker cells tend to alternate faster than the Hadley cell, their decadal resonant frequency is consistent with anomalous north–south displacements of the near-equatorial trough and wet–dry cycles of Ethiopian rainfall.

4 Conclusions

Ethiopian decadal climate variability has been characterized in this study. There are two distinct rainfall modes that correspond with unique seasonal cycles and opposing responses to regional and global forcing. The northern zone that impacts the Nile River and underlies the tropical easterly jet has a unimodal rainy season that is enhanced by an AMO SST pattern in warm phase. This northern mode links with the Atlantic Walker zonal overturning circulation (PSI-1) and has exhibited 10–12-year cycles through much of the twentieth century. The southern zone has a bimodal rainy season (mode 2) that is enhanced by a PDO SST pattern in cool phase and the southern Hadley meridional overturning circulation. Multiyear wet and dry spells were uncovered in Ethiopian rainfall records. The wet periods were: 1962–1966, 1979, 1998–1999, and 2006–2007; dry periods included 1971–1973, 1984–1986, 1992, and 2002–2004. Decadal climate oscillations require attention because of their effect on food and water resources. It is possible for agrarian communities to set aside resources for one "bad" year, but more than two in a row leads to socioeconomic disruption. Prediction of the amplitude and timing of multiyear wet and dry spells is possible given that the Walker and Hadley signals tend to lead SST and rainfall by over 1 year (Fig. 6). Further efforts to better understand and predict the variable climate of Ethiopia will involve relating intra-seasonal weather events to the background climate and determining how localized land-atmosphere feedbacks conspire with remote teleconnections.

Fig. 9 Vertical sections of SVD loading pattern for mode-1 a zonal wind (U1w) across longitudes averaged 5° S–10° N, b meridional wind across latitudes (V1h) averaged 60° W–90° E, and c their time scores with V1h-inverted. African highlands are represented by *shaded rectangle*

References

Barlow M, Nigam S, Berbery EH (2001) ENSO, Pacific decadal variability, and U.S. summertime precipitation, drought, and stream flow. J Climate 14:2105–2128

Bretherton CS, Smith C, Wallace JM (1992) An intercomparison of methods for finding coupled patterns in climate data. J Climate 5:541–560

Camberlin P (1995) June-September rainfall in Northeast Africa and atmospheric signals over the tropics: a zonal perspective. Int J Climatol 15:773–783

Camberlin P (1997) Rainfall anomalies in the source region of the Nile and their connection with Indian summer monsoon. J Climate 10:1380–1392

Camberlin P, Janicot S, Poccard I (2001) Seasonality and atmospheric dynamics of the teleconnection between African rainfall and tropical sea surface temperature: Atlantic vs. ENSO. Int J Climatol 21:973–1005

Charney JG (1975) Dynamics of desert and drought in the Sahel. Quart J Royal Meteorol Society 101:193–202

Conway D, Mould C, Wolde AB (2004) Over one century of rainfall and temperature observations at Addis Ababa, Ethiopia. Intl J Climatol 24:77–91

Eltahir EAB, Wang G (1999) Nilometers. El Nino and climate variability. Geophys Res Lett 26(4):489–492

Enfield DB, Mestas-Nunez AM, Trimble PJ (2001) The Atlantic Multidecadal Oscillation and its relationship to rainfall and river flows in the continental US. Geophys Res Lett 28:2077–2080

Folland CK, Palmer TN, Parker DE (1986) Sahel rainfall and world-wide sea temperature, 1901–85. Nature 320:602–607

Fontaine B, Janicot S, Moron V (1995) Rainfall anomaly patterns and wind field signals over West Africa in August 1958–1989. J Climate 8:1503–1510

Fontaine B, Trzaska I, Janicot S (1998) Evolution of the relationship between near global and Atlantic SST mode and the rainy season in West Africa: statistical analyses and sensitivity experiments. Climate Dynamics 14:353–368

Glantz MH (1996) Currents of change: El Nino's impact on climate and society. Cambridge University Press, Cambridge, p 194

Glantz MH, Katz RW, Nicholls N (1991) Teleconnections linking worldwide climate anomalies: scientific basis and societal impact. Cambridge University Press, Cambridge, p 535

Hammer GL, Nicholls N, Mitchell C (2000) Applications of seasonal climate forecasting in agricultural and natural ecosystems: the Australian experience. Kluwer, Dordrecht, pp 149–160

Hastenrath S (2000) Interannual and longer-term variability of upper air circulation over the tropical Atlantic and West Africa in boreal summer. Intl J Climatol 20:1415–1430

Jury MR (2002) Development of statistical forecast models of summer climate and hydrological resources over Southern Africa. Water Res Comm. Report 903/1/02, Pretoria, pp 116

Jury MR, Huang B (2004) The Rossby wave as a key mechanism of Indian Ocean climate variability. Deep-Sea Res 51:2123–2136

Jury MR, Mulenga HM, Mason SJ, Brandao A (1997) Development of objective statistical system to forecast summer rainfall over southern Africa. WRC Report 672/1/97, Pretoria, pp 45

Kalnay E et al (1996) The NCEP/NCAR 40-year reanalysis project. Bull Am Meteorol Soc 77:437–471

Lamb PJ (1978) Large-scale tropical Atlantic circulation patterns associated with Subsaharan weather anomalies. Tellus 30:240–251

Lamb PJ (1982) Persistence of Subsaharan drought. Nature 299:46–48

Lin YL, Robertson KE, Hill CM (2005) Origin and propagation of a disturbance associated with an African easterly wave as a precursor of hurricane Alberto (2000). Mon Wea Rev 133:3276–3298

Lough JM (1986) Tropical Atlantic seas surface temperatures and rainfall variations in sub-saharan Africa. Mon Wea Rev 114:561–570

Lyon B, Mason SJ (2009) The 1997–98 summer rainfall season in Southern Africa. Part II: model simulations and coupled model forecasts. J Climate 22(13):3802–3818

Moura AD, Sarachik ES (1997) Seasonal-to-interannual climate prediction and applications: new institutions, new possibilities. WMO Bull 46(4):342–347

Nicholson SE (1981) Rainfall and atmospheric circulation during drought periods and wetter years in West Africa. Mon Wea Rev 109:2191–2208

Nicholson SE (1998) Decadal rainfall variability of rainfall over Africa in the past two centuries, Water resources variability in Africa. Proc Intl Assoc Hydrol Sci 252:107–116 Abidjan

Nicholson SE, Palao IM (1993) A re-evaluation of rainfall variability in the Sahel. Part I: Characteristics of rainfall fluctuations. Int J Climatol 13:371–289

Nicholson SE, Grist JP (2001) A conceptual model for understanding rainfall variability in the West African Sahel on internnual and interdecadal timescale. Int J Climatal 21:1733–1757

Palmer TN (1986) Influence of Atlantic, Pacific, and Indian Oceans on Sahel rainfall. Nature 322:251–253

Quinn WH (1992) A study of southern oscillation-related climate activity 622-1990 incorporating Nile river flood data. In: Diaz HF, Markgraf V (eds) "El Nino: historical and paleoclimae aspects of Southern Oscillation". 119-142

Rudolf B, Schneider U (2005) Calculation of gridded precipitation data for the global land-surface using in-situ gauge observations, Proc Intl Precip Working Group, Monterey, Eumetsat contribution ISBN 92-9110-070-6

Segele ZT, Lamb PJ, Leslie LM (2009) Seasonal-to-interannual variability of Ethiopia/Horn of Africa monsoon. Part I: Associations of wavelet-filtered large-scale atmospheric circulation and global sea surface temperature. J Climate 22:3396–3421

Seleshi Y, Demarée GR, Delleur JW (1994) Sunspot numbers as a possible indicator of annual rainfall at Addis Ababa Ethiopia. Intl J Climatol 14:911–933

Semazzi HFM, Burns B, Lin NH, Schemm JE (1996) A GCM study of teleconnections between the continental climate of Africa and global sea surface temperature. J Climate 9:2480–2497

Shanko D, Camberlin P (1998) The effect of southwest Indian Ocean tropical cyclone on Ethiopian drought. Int J Climatol 18:1373–1388

Smith TM, Reynolds RW, Peterson TC, Lawrimore J (2008) Improvements to NOAA's historical merged land-ocean surface temperature analysis (1880–2006). J Climate 21:2283–2296

Tourre YM, Kushnir Y, White WB (1999) Evolution of interdecadal variability in sea level pressure, sea surface temperature and upper ocean temperature over the Pacific Ocean. J Phys Oceanogr 29:1528–1541

Venegas SA (2001) Statistical methods for signal detection in climate. Danish Centre for Earth System Science, Niels Bohr Inst Astronomy and Geophysics, Univ. Copenhagen, Denmark, p 96

von Storch H, Navarra A (1995) Analysis of climate variability—applications of statistical techniques. Springer, New York, p 334

Wang G, Eltahir EAB (1999) Use of information in the medium- and long-range forecasting of the Nile floods. J Climate 12:1726–1737

WCRP (1999) A strategy for climate research in Africa. World Climate Research Programme, CLIVAR. WRCP Report 16/1999. ICPO Publication Series 29

Wood CA, Lovett R (1984) Rainfall, drought and the solar cycle. Nature 251:594–596

Xie S-P, Annamalai H, Schott FA, McCreary JP (2002) Structure and mechanisms of south Indian Ocean climate variability. J Climate 15:864–878

Xue Y, Liu KN, Kasahara A (1990) Investigation of bio-geophysical feedback on African climate using a two-dimensional model. J Climate 3:337–352

Yeshanew A, Jury MR (2007) North African climate variability, part 2: tropical circulation systems. Theor Appl Climatol. doi:10.1007/s00704-006-0243-7

Zeng N, Eltahir EAB (1998) The role of vegetation in the dynamics of West African monsoons. J Climate 11:2078–2096

Zeng N, Neelin JD, Lau KM, Tucker CJ (1999) Enhancement of interdecadal climate variability in the Sahel by vegetation interaction. Science 286:1537–1540